

Diffusivity in Novel Diamine-Based Water-Lean Absorbent Systems for CO₂ Capture Applications

Yanjie Xu, Qi Yang, Graeme Puxty, Hai Yu, William Conway, Mengxiang Fang, Tao Wang,* and Roger J. Mulder*



Cite This: *Ind. Eng. Chem. Res.* 2022, 61, 12493–12503



Read Online

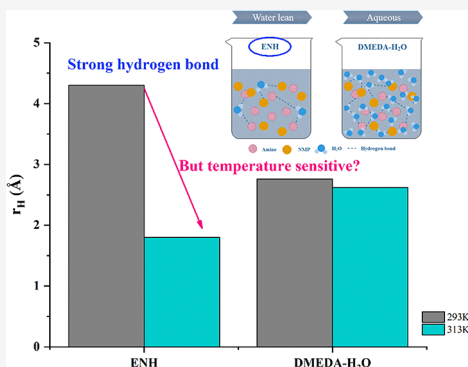
ACCESS |

Metrics & More

Article Recommendations

Supporting Information

ABSTRACT: Significant reduction of the water content of traditional absorbents, increasing organic character of absorbent molecules, and substitution of water with a non-aqueous diluent are increasingly attracting interest as means to improve absorbent performance. From our previous work, the novel diamine absorbents *N,N*-dimethyl-1,3-propanediamine (DMPDA) and *N,N*-dimethyl-1,2-ethanediamine (DMEDA), also utilizing *N*-methyl-2-pyrrolidone (NMP) as a non-aqueous diluent to reduce the water content of the absorbent, were demonstrated to produce an absorbent blend with a significantly lower overall energy consumption (for CO₂ regeneration). Alongside the thermodynamic performance, CO₂ absorption mass transfer plays an equally critical role in the overall performance of an absorbent for CO₂ capture processes. Gaining an understanding of the fundamental factors influencing mass transfer behavior has long been the focus of research efforts, and the diffusivity of the absorbent molecules is a critical factor for amines to be able to rapidly react with CO₂. Expanding on the initial investigation of these promising blends, we evaluate herein the diffusivity of the component molecules of a number of blends as a function of temperature, CO₂ loading, absorbent composition, and absorbent viscosity. A powerful technique based on nuclear magnetic resonance (NMR) spectroscopy was used to provide direct measurement of the diffusion coefficients of individual chemical species in the blends. Diffusivity and viscosity were found to behave very differently in water-lean and aqueous blends, with water-lean blends being particularly sensitive to CO₂ loading and water content. The hydrodynamic radii of species in the water-lean blends were particularly sensitive to temperature relative to the aqueous blends, significantly decreasing as the temperature was increased with associated potential mass transfer benefits. This can be put down to the introduction of NMP, which weakens the intermolecular interactions (forming a hydrogen bond) between molecules and water, and this impact increased through increasing temperature. This highlights that the optimal operating conditions for water-lean blends are likely quite different to those used traditionally for aqueous blends.



1. INTRODUCTION

The amount of carbon dioxide released globally in 2020 from the combustion of fossil fuels was *ca.* 34.0 Gt,¹ decreasing by ~7.0% below 2019 levels due to the slowdown and impacts of the COVID-19 pandemic. While this observed reduction in emissions is not yet sustainable in the long term, at least in the short term, it clearly demonstrates that the magnitude of the impact humanity is capable of having on its overall CO₂ emission profile and, subsequently, its effort to reduce the effects of climate change are confirmed to be observable and substantial if achieved. Carbon capture, utilization, and storage (CCUS) is regarded as one of the key approaches capable of significant reductions in CO₂ emissions from fossil fuel-based combustion processes, but more importantly into the future is the role CCUS technologies will play in abatement of CO₂ emissions from heavy industry where few emission abatement options currently exist. CO₂ capture using typical amine-based aqueous absorbents such as monoethanolamine (MEA), 2-amino-2-methylpropanol (AMP), and piperazine (PZ) is the

leading capture technology but continues to face technical challenges on its way to global adoption at the necessary industrially relevant and economically palatable scale. Much of the improvement must target the low cyclic capacity and high overall energy consumption of the absorbents such as that seen in MEA processes,^{2–6} elevated volatility and viscosity in AMP blends,^{7–9} and the formation of solid precipitates at lower temperatures with PZ,^{10–12} as examples.

A recent momentum shift of the fundamental research from typical aqueous absorbent systems toward novel water-lean and non-aqueous absorbents is expected to offer a considerable energy improvement over the aqueous absorbent systems,

Received: June 6, 2022

Revised: July 30, 2022

Accepted: August 1, 2022

Published: August 11, 2022



ideally without significant modification to traditional CO₂ capture absorbent designs or infrastructure. The introduction of alcohols,^{13–16} *N*-methyl-2-pyrrolidone (NMP),^{17–20} or sulfolane (SFL)^{21–23} to reduce the aqueous nature of amine-based absorbent blends has been observed to result in lower latent heats of regeneration. A 45% decrease in energy consumption was observed in water-lean blends of amino acid salts and 2-alkoxyethanols compared with aqueous MEA.²⁴ A non-aqueous solvent containing AMP, 2-(2-aminoethylamino) ethanol (AEEA), and *N*-methyl pyrrolidone (NMP) was developed with a lower regeneration energy (2.09 GJ·t^{−1} CO₂).²⁵ Hellebrant *et al.* also reported that modification of non-aqueous “antisolvents” such as hexadecane assisted in the chemical desorption chemistry of CO₂ from a loaded (CO₂) solution of a CO₂-binding organic liquid (CO₂BOL). This modification achieved a temperature decrease from traditional 90 °C to 73.0 °C during the solvent regeneration step of their process.²⁶ Notably and importantly, the reduction in regeneration temperature consequently reduced solvent attrition via thermal degradation.²⁷ Similarly, Wang *et al.* employed a phase-separating absorbent comprising a mixture of diethylenetriamine (DETA) and sulfolane as an alternative to aqueous MEA, resulting in a reduction of the total heat duty by up to 19.0%.²²

To date, few studies have invested significant efforts into the understanding of mass transfer processes occurring within water-lean absorbents. Among the fundamental properties influencing the mass transfer performance are the physical properties of the absorbents including the diffusion coefficients and hydrodynamic radii, which play key roles in the fundamental CO₂ capture chemistry. In a recent pioneering study, Yuan and Rochelle built a kinetic model to compile and understand the effects of absorbent properties on CO₂ mass transfer in an MEA-NMP-water absorbent.¹⁷ Initially, their mass transfer model suggested that the CO₂ diffusion into and subsequent reaction within aqueous MEA can be approximated by pseudo-first order (PFO) behavior, while the addition of NMP causes deviation from PFO conditions by negatively enhancing depletion of MEA on the surface. The study also concluded that the semi-aqueous absorbent demonstrated an excellent CO₂ absorption rate; however, the increased viscosity reduced heat transfer, which negatively impacts heat exchanger performance. Wang *et al.* also observed that the CO₂ mass transfer coefficient in their DETA-sulfolane absorbent decreased with increasing CO₂ uptake, which they attributed to the corresponding increase in the viscosity of the solution.²²

The bulk of previous mass transfer and diffusion studies in water-lean or non-aqueous CO₂ capture absorbents typically involves ionic liquids. The effects of anion selection in three 1-butyl-3-methylimidazolium ([bmim]⁺)-based ionic liquids on kinetic and thermodynamic performances were illustrated by Gonzalez-Miquel *et al.*, in which bmim tris(pentafluoroethyl)trifluorophosphate ([bmim][FAP]) showed the ideal solubility of those investigated, while bmim bis(trifluoromethanesulfone)imide ([bmim][NTf₂]) performed better in diffusivity.²⁸ Similar impacts are expected in water-lean and non-aqueous blends due to the presence of ions (in the form of carbamates, carbonates, and protonated amines). This phenomenon also demonstrates that both kinetics and thermodynamics are critical properties to be considered in absorbent selection.

Viscosity shows a strong negative influence on diffusivity and, thus, the mass transfer performance of an absorbent. A

primary amine-functionalized ionic liquid, 1-(3-aminopropyl)-3-methylimidazolium tetrafluoroborate ([APmim]BF₄), has some 1.0–3.0 orders of magnitude reduction in the diffusion coefficient compared with MEA in an aqueous solution, and the reduction correlated with the elevated viscosity in the ionic liquid.²⁹ It is found that the viscosity of 1-alkyl-3-methylimidazolium tricyanomethane ionic liquids ([C_nmim][TCM], *n* = 2, 4, 6, 7, and 8) surprisingly decreased upon absorption of CO₂, leading to an enhanced diffusion coefficient, which shows significant promise for utilization of this phenomena in industrial applications.³⁰ A viscosity of 124.0 mPa·S^{−1} was obtained for an *N,N*-dimethyl-*N*-(2-methoxyethyl) ethylenediamine (MeO-DMEDA)-based non-aqueous absorbent at its maximum CO₂ loading (0.7 mole CO₂·mole amine^{−1}).³¹ While it is still high compared to that of aqueous MEA³² (2.7 mPa·S^{−1} with 0.5 mole CO₂·mole amine^{−1} at 40.0 °C), this is a substantial improvement for these water-lean absorbents and positions them for further investigations.

In an expansion of our previous work on the thermodynamic behavior and enhanced energy performance of two diamine-based water-lean absorbents, *N,N*-dimethyl-1,3-propanediamine (DMPDA) and *N,N*-dimethyl-1,2-ethanediamine (DMEDA), in blends with the organic component NMP,^{33,34} here, we investigate the DMEDA and DMPDA blends with NMP with a water content of less than 20% (5, 10, and 20%) and CO₂ loadings and the changes in their viscosity and diffusivity as a pathway to understanding the impacts of the blend properties on CO₂ absorption mass transfer. Utilizing NMR spectroscopy as an analytical method here allows for a more controlled and consistent evaluation of diffusion compared with other laboratory techniques including thermogravimetric analysis,^{35–37} thin liquid film methods,^{38,39} Fourier transform infrared spectroscopy,⁴⁰ and Taylor dispersion method⁴¹ and/or modeling methods that rely on empirical relationships.^{42,43} MEA and its corresponding water-lean absorbent blends have been included in the suite of absorbent blends investigated here for comparison.

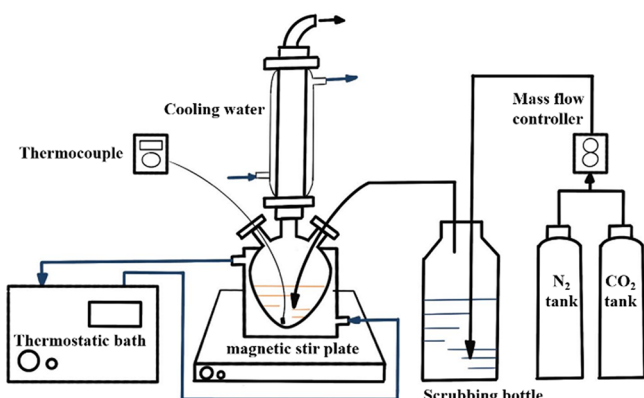
2. EXPERIMENTAL SECTION

2.1. Chemicals. Carbon dioxide (CO₂, 99.9%) and nitrogen (N₂, 99.9%) gases were supplied by BOC Australia. Abbreviations and molecular structures of amines and cosolvents utilized in this study are displayed in Table 1. Monoethanolamine (MEA, 99%, Merck), *N,N*-dimethyl-1,2-ethanediamine (DMEDA, 99%, Sigma), *N,N*-dimethyl-1,3-propanediamine (DMPDA, 99%, Aldrich), and 1-methyl-2-pyrrolidone (NMP, 99%, ChemSupply) were all used as received without additional purification. Deionized water was used to prepare all solutions containing water as a blend component. The concentration of amines in each blend remains as 30%, and the different quantities of *N*-methyl-2-pyrrolidone and water make the remaining 70% of components. The compositions of water-lean solvents studied in this work are shown in Table S1 with their abbreviations. The abbreviation contains the amine type (fixed at 30% w/w) and the water fraction as % w/w. The NMP fraction is inferred as it is (70 H₂O) % w/w.

2.2. CO₂ Absorption Equilibrium. The apparatus used for CO₂ absorption is shown schematically in Figure 1 and described in detail in our previous paper.^{33,34} The equilibrium flask was charged with the absorbent mixture after which a CO₂/N₂ gas mixture, presaturated with water, was bubbled

Table 1. Structures and Abbreviations of Amine Components and Cosolvents

Name	Abbreviation	Structure
Monoethanolamine	MEA	
<i>N,N</i> -dimethyl-1,2-ethanediamine	DMEDA	
<i>N,N</i> -dimethyl-1,3-propanediamine	DMPDA	
1-methyl-2-pyrrolidone	NMP	

**Figure 1.** Schematic diagram of the CO_2 absorption apparatus used in this work.

through the solution for approximately 24 h until it was saturated with CO_2 . A range of CO_2 loadings was obtained by dilution of the CO_2 -rich solution with a CO_2 -free absorbent with the samples then prepared for analysis by NMR spectroscopy.

2.3. Viscosity Measurements. Viscosities of the various CO_2 -loaded solutions were measured in duplicate using an Anton Paar Automated Micro-viscometer at 298.0 and 313.0 \pm 0.1 K. The resulting values are reported as the average of the duplicate measurements.

2.4. NMR Spectroscopy. NMR measurements were performed on a suite of Bruker Avance 400 and 500 MHz NMR spectrometers with the samples held at their specified temperatures to within \pm 0.1 K. ^1H and ^{13}C chemical shifts were referenced to 13.0% trioxane in deuterium oxide located within a sealed glass capillary inside the NMR tube (reference chemical shift at 93.52 ppm for ^{13}C and 5.09 ppm for ^1H signals). The CO_2 loadings of samples were quantified from

the ^{13}C NMR spectra collected with inverse-gated ^1H decoupling at a pulse angle of 30° (zgig30 pulse program, Bruker) as the sum of 32 scans with a relaxation delay (AQ + D1) greater than 5× the longest measured T_1 in the molecule. Both the ^1H and ^{13}C 90° pulse lengths were measured for each sample.

Diffusion coefficients were determined using the pulsed field gradients spin echo method^{44,45} utilizing a Bruker Avance 500 NMR spectrometer equipped with a 5 mm probe operating with a 5.35 G/mm z -gradient. Bruker's Topspin 3.6 software was utilized for spectral acquisition and post-processing. At least 30 min was allowed for each sample to reach thermal equilibrium within the NMR spectrometer prior to spectral acquisition. The NMR spectra were measured with a stimulated echo sequence with one spoil gradient. The diffusion time (Δ) of 100 ms was used, and the gradient pulse length (δ) was determined for each of the various measurement temperatures. Gradient pulses exhibited a smoothed square chirp shape. Experiments were performed as pseudo-2D with a linear variation of the gradient from 2.0 to 95.0% of the maximum intensity in 32 steps. Subsequent spectral data were processed and the peak areas I were used to fit the Stejskal-Tanner equation (eq 1)^{46,47} to determine the diffusion coefficient D as single-component fits.

$$I = I_0 e^{-D(2\pi/\delta)^{1/2}[(\Delta-\delta)/3] \times 10^4} \quad (1)$$

The resulting diffusion coefficient for each of the observed species including amine, carbamate, carbonate, and water is available in Figures S1–S3 of the Supporting Information and will be discussed in the following sections.

3. RESULTS AND DISCUSSION

3.1. Diffusion Coefficient. The gradient ^1H NMR spectral data were used to calculate diffusion coefficients D for each of the absorbent series at various CO_2 loadings and three temperatures (293.0, 303.0, and 313.0 K). For each system, the values for four species including H_2O , NMP, amine, and carbamate were obtained. The water-lean systems displayed a high level of consistency within the trends responding to the changes in temperature, NMP/water ratio, and CO_2 loading. Single representative measurements are discussed herein. The comprehensive suite of the resulting NMR data with variations in temperature, NMP/water ratio, and CO_2 loading is available in Figures S1–S3 in the Supporting Information.

3.1.1. The Effect of Temperature and CO_2 Loading on Amine Diffusion: General Trends. The effect of CO_2 loading and temperature on diffusion in three amine absorbent blends with 5.0% H_2O is shown in Figure 2a,b, respectively. Similar trends in the observed diffusivities with increasing temperature and CO_2 loading are apparent among absorbent systems with different water contents. For simplicity, the general trends in this section will initially be discussed here using the data for the 5.0% H_2O series. From Figure 2a, diffusion coefficients here increased with increasing temperature for a given CO_2 loading and for each blend. Moreover, it was found that the diffusion coefficient was linearly correlated with $3/2$ power of temperature (K), for which a similar trend has been reported in gaseous systems previously.⁴⁸ The linear relation between $T^{3/2}$ and D is displayed in Figure 2b. Importantly, it is worth noting that both the aqueous and water-lean absorbents demonstrated this highly linear relationship.

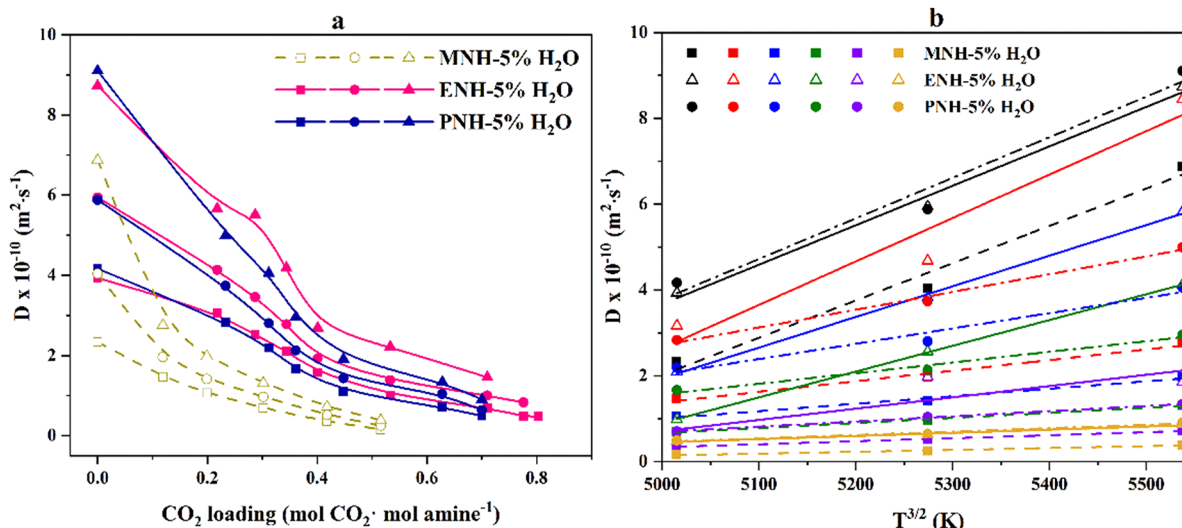


Figure 2. (a) Diffusion coefficients of amine versus CO_2 loading at different temperatures in three amine-based absorbents with 5% H_2O (square: 293.0 K; circle: 303.0 K; triangle: 313.0 K). (b) Diffusion coefficient of amine versus $3/2$ power of temperature in three amine-based absorbents with different CO_2 loadings (dotted line: MNH-5% H_2O ; solid line: ENH-5% H_2O ; dotted and dashed line: PNH-5% H_2O).

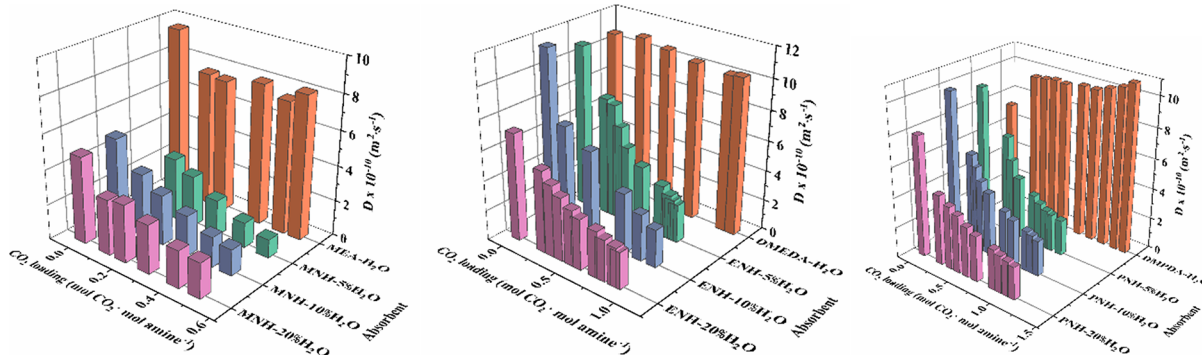


Figure 3. Diffusion coefficients of H_2O versus CO_2 loading at 313.0 K in three amine-based absorbent series.

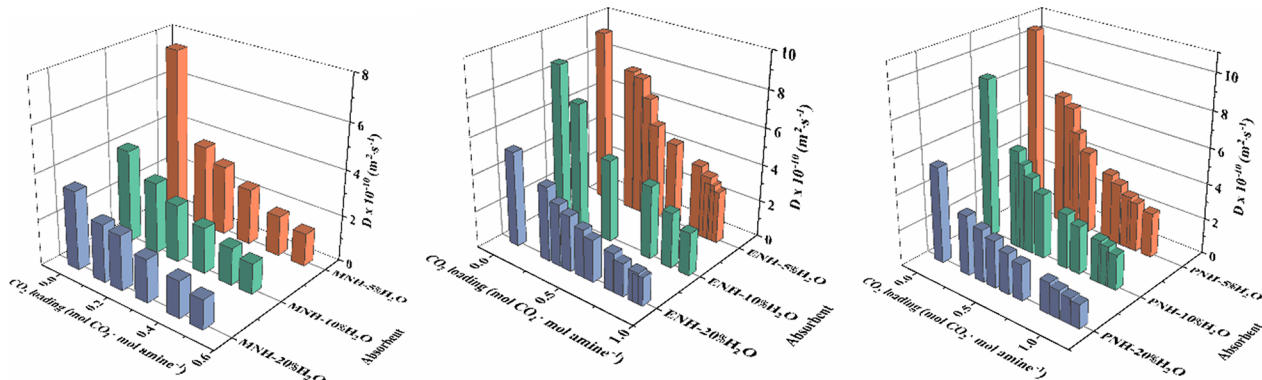


Figure 4. Diffusion coefficients of NMP versus CO_2 loading at 313.0 K in three amine-based absorbent series.

In terms of CO_2 loading, there is a general trend with decreasing diffusion coefficient and increasing CO_2 loading. The major variation of the absorbent system in a CO_2 absorption process is the change in the chemical composition with increasing amounts of CO_2 absorbed as carbamates, carbonates, and protonated amines. In its simplest form, the formation and presence of charge(s) on these species (resulting from the reaction with CO_2) hinder the movement of the molecules (themselves and others within the solution), naturally leading to a decline in the diffusion coefficients.

3.1.2. The Effect of Different Species in Liquid. Expanding on the simple amine data in the previous section, the individual species diffusion coefficient data for the different amine systems at 313.0 K, being a typical CO_2 absorption temperature, are displayed in Figures 3 and 4.

Figures 3 and 4 show the diffusion coefficients of the two main nonreactive absorbent components H_2O and NMP with increasing CO_2 loading at 313.0 K. It is immediately apparent that the diffusivity of H_2O is distinctly different in the aqueous system to that in the water-lean systems. The diffusivities of

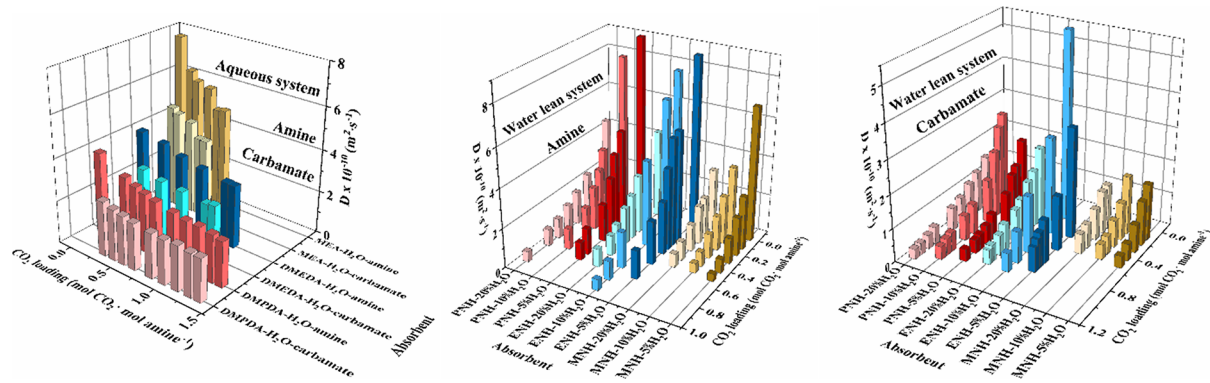


Figure 5. Diffusion coefficients of amine and carbamate versus CO_2 loading at 313.0 K in three amine-based absorbent series.

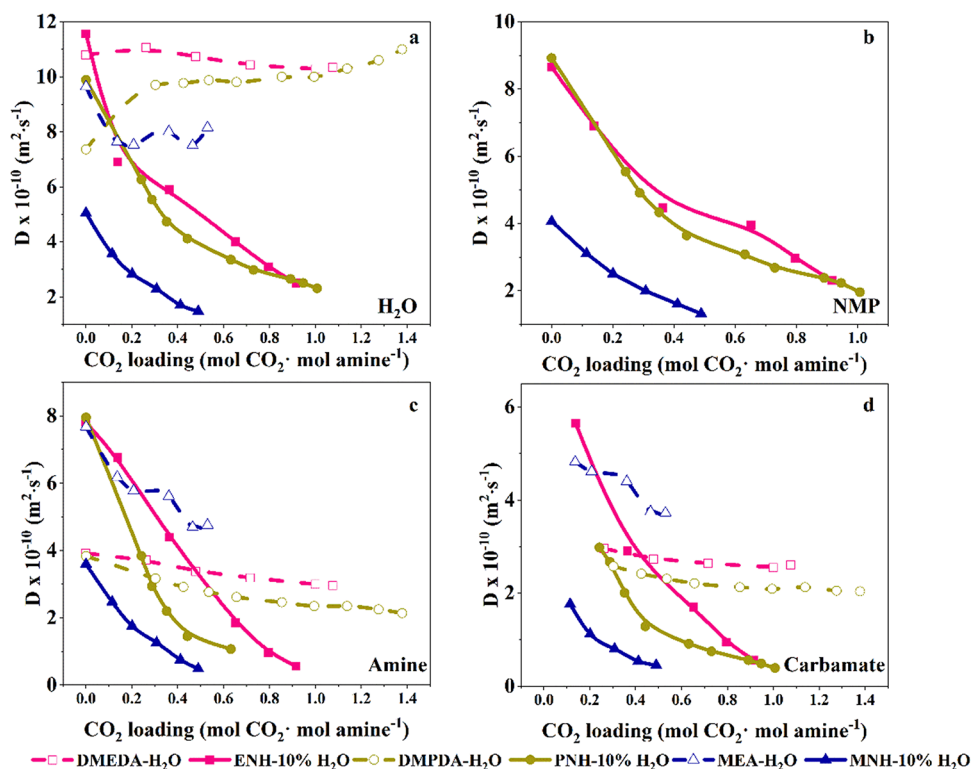


Figure 6. Comparison on the diffusivity of four species in three water-lean absorbents with 10% H_2O and their corresponding aqueous absorbents at 313.0 K (a: H_2O ; b: NMP; c: amine; d: carbamate).

H_2O in the absence of NMP are relatively constant with increasing CO_2 loading in each of the blend systems, while for the corresponding water-lean absorbents, there is a marked decrease with CO_2 loading. It can be explained that a huge amount of free H_2O in these three aqueous absorbents weakens the impact of carbamate, carbonate, and protonated amine formed through CO_2 uptake on the diffusivity of H_2O . The diffusivity of water in the MEA blends at zero CO_2 loading decreases substantially with the addition of NMP by up to ~50%. The trends for DMEDA and DMPDA are less obvious with the diffusivity of water fluctuating around the initial value for the CO_2 free blends, only decreasing below the initial value for DMEDA, with DMPDA essentially remaining constant. The diffusivity of H_2O decreases with increasing CO_2 loading in water-lean absorbents. Using the data for blends containing the largest amount of H_2O , the diffusivity of H_2O decreases by about 50% or so for the MEA, DMEDA, and DMPDA blends. Interestingly, the diffusivity of H_2O was

found to be comparable at CO_2 loadings <0.2 ($\text{mol CO}_2 \cdot \text{mol amine}^{-1}$) across the three MEA blends containing differing amounts of H_2O , while the blend with the highest H_2O content (20%) maintained the largest H_2O diffusivity as the CO_2 loading increased toward saturation. The change in H_2O diffusivity may result from strong hydrogen bonding between H_2O and the amine and carbamate and the interruption of the hydrogen bonding network (via H_2O) with increasing concentration of the NMP component into the blend. H_2O diffusivity in the two diamine absorbents, DMEDA and DMPDA, was the highest in the blends with the lowest content of H_2O over the entire CO_2 loading range (similar to 10% water content in zero loading). Again, in each of the blends, the water content has a positive influence on hydrogen bond formation in the water-lean system.³⁴

Diffusion of NMP followed similar trends to the diffusion of H_2O with increasing CO_2 loading (Figure 4). A similar diffusion coefficient for NMP was achieved in the MEA blends

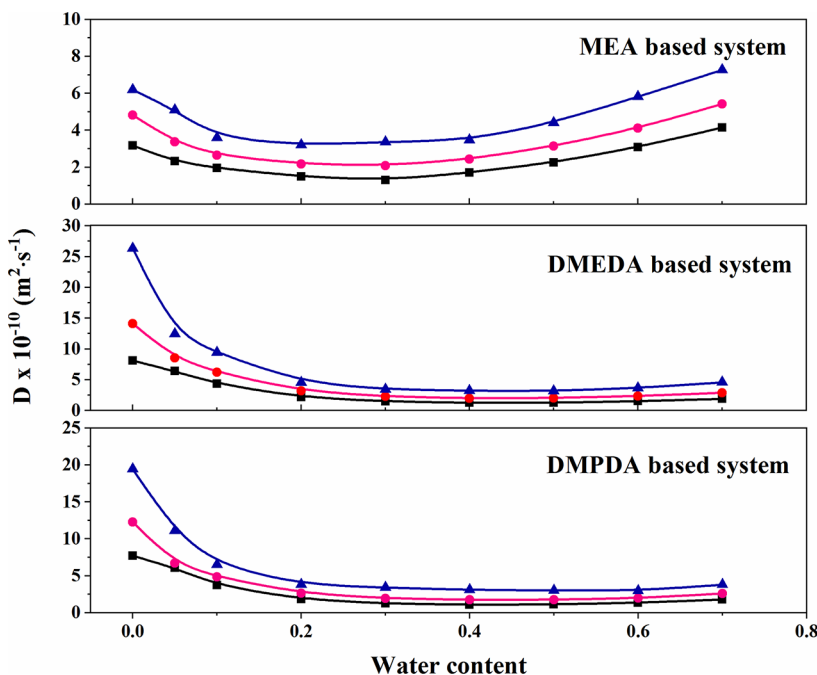


Figure 7. Diffusivity of amine in three amine-based absorbent series with a fully covered water ratio at three temperatures (black: 293.0 K; red: 303.0 K; blue: 313.0 K).

with differing H₂O, below 10% H₂O, while the range and spread of values in the two diamine systems were wider. This effect could result from the difference in the chemical structure of MEA with the hydroxyl group (in MEA), which is able to form a stronger hydrogen bond with H₂O compared to the amino groups in the diamine. Hence, it is the strong attraction between MEA (via OH) and H₂O stemming the diffusivity of H₂O, leading to a lower diffusion coefficient (of H₂O) than that of NMP.

Diffusion coefficients of amine and carbamate as a function of CO₂ loading at 313.0 K in the three amine blend systems are displayed in Figure 5. Similar to the diffusivity of H₂O, amine, and carbamate, diffusivities in the absence of NMP are only slightly changed with increasing CO₂ loading. However, in the presence of NMP, the trend in diffusivity decreases significantly with increasing CO₂ loading. The diffusivity of amine and carbamate in the MEA-H₂O mixtures was about 50% greater than that in the corresponding DMEDA-H₂O and DMPDA-H₂O blends. In the case of the MEA blend, addition of NMP resulted in a decrease in the diffusivity of amine and carbamate. Interestingly, the diffusivity of amine in the DMEDA and DMPDA blends in the presence of NMP initially exceeds that of the purely aqueous solutions in the low CO₂ loading range, indicating a positive impact of the addition of NMP. This enhancement of diffusion transitions around the mid-CO₂ loading range at 0.5 mol CO₂·mole amine⁻¹ where it decreases substantially. The trends in diffusivity of the amine between the DMEDA and DMPDA series are similar, with the former maintaining a slightly elevated and more linear decrease in diffusion coefficient over the CO₂ loading range. This is compared to DMPDA, which was observed to decrease more rapidly in the initial CO₂ loading range, where the rate of change begins to taper in the CO₂ loading beyond 0.5 mol CO₂·mol amine⁻¹ and approaches saturation. It is clear from the trends that the additional length in the carbon chain from DMEDA to DMPDA, despite being only a single carbon, has a

dramatic effect on the diffusivity. Similar phenomena were also observed in the diffusivity curves of the carbamate in each of the blends. The observed phenomena may be due to the larger size of the carbamate and the formation of protonated carbamate species ((CH₃)₂⁺HN-(CH₂)_x-NH-COO⁻, x = 2 or 3).

3.1.3. Difference in Diffusivity between Absorbents. To clearly demonstrate the difference between the MEA, DMEDA, and DMPDA systems, diffusivities of the four species, H₂O, NMP, amine, and carbamate, in each of the blends with 10% H₂O at 313.0 K are shown in Figure 6. The diffusion coefficients of H₂O follow similar trends among the aqueous absorbents MEA, DMEDA, and DMPDA across the CO₂ loading range and follow the order DMEDA ≈ DMPDA > MEA. Surprisingly, H₂O had the lowest diffusion in MEA. However, the larger concentration of MEA in the absorbent (5 mol·L⁻¹) and the presence of the strongly hydrogen bonding hydroxyl group (of MEA) significantly impact the diffusion of H₂O. NMP diffusion in the absorbents followed the trend DMEDA ≈ DMPDA > MEA, showing greater diffusivity in the presence of DMEDA and DMPDA as opposed to MEA. Amine diffusivity was the largest for aqueous MEA and the DMEDA and DMPDA blends in the presence of NMP at CO₂ loadings <0.5 mol CO₂·mol amine⁻¹. Then, the rate of decrease (in diffusivity) was similar for the above three blends, maintaining similar diffusivity with CO₂ loading from 0.1 to 0.4 mol CO₂·mol amine⁻¹. Notably, diffusivity in the DMEDA and DMPDA blends with NMP was approximately double those of the corresponding aqueous blends initially, decreasing to similar values approaching 0.5 mol CO₂·mol amine⁻¹. Similar to H₂O and NMP, the diffusivity of MEA in the presence of NMP was impacted dramatically, having the lowest values of the blends evaluated here over the entire CO₂ loading range. Carbamate followed similar trends to that of the amine, which is expected given the similar chemical structures.

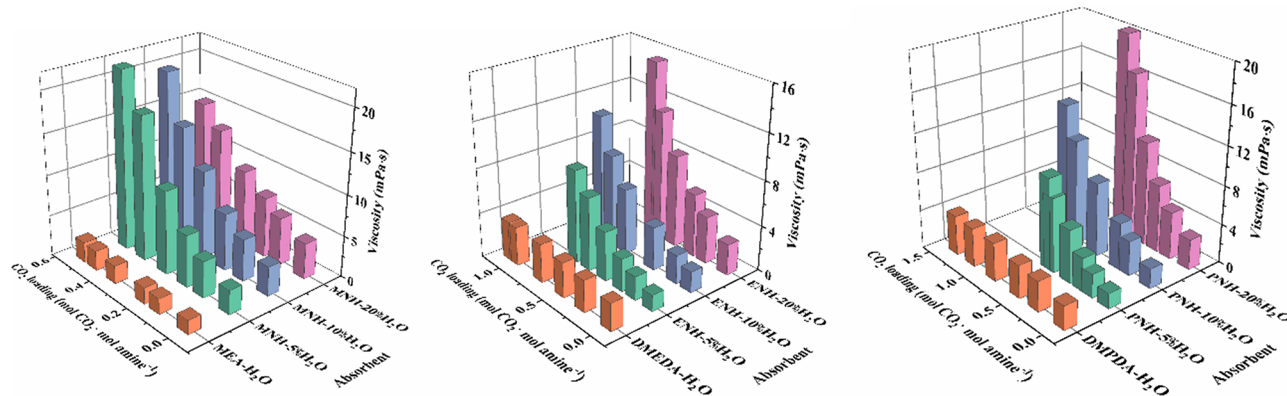


Figure 8. Measured viscosity versus CO₂ loading of three amine absorbents at 313.0 K.

3.1.4. Effect of Water Content. To further understand the impact of water content on diffusivity, a wider range of water ratios (from 0.0 to 70.0% w/w) was evaluated here at three temperatures with the amine content maintained at 30% w/w and the NMP content at 70% H₂O w/w. The resulting diffusivities of amine in the three blends under CO₂-free conditions are shown in Figure 7. As would be expected, the diffusivity increases with increasing temperature. The trend with increasing water content is similar at each temperature.

It is also noticeable that all three amines had high diffusivity in the blend with NMP (0% H₂O). Then, the diffusivity decreased, while the water contents increased. These trends differed when the water contents in blends were over 30%. With a further increase in water content beyond this point, the diffusivity of two diamines relatively remained steady, while that of MEA started increasing and reached the highest value in its aqueous solution (70% H₂O).

To explain the results, it is worth referring the molecular structures of the involved compounds. Both diamines contain one primary and one tertiary amino group, while MEA has one primary amino and one hydroxyl group. So, MEA has a stronger ability to form hydrogen bonds and greater hydrophilicity than diamines.⁴⁹ NMP is a nonprototonic polar molecule that generally does not form hydrogen bonds, but its amide group can be affected by the electron polarity of other molecules, although it is much weaker than hydrogen bonds. The water component is the most common polar liquid with a strong ability to form hydrogen bonds. In the NMP blends (0% H₂O), all three amines have a smaller interaction with NMP, hence moving reasonably easier than in the situation with up to 30% added water. The added water should form hydrogen bonds with amino and hydroxyl groups of amines. The water ends of these hydrogen bonds can attract the polar amide group of NMP, hence making the amine shift slower in the blends. After the amine molecule was fully hydrated and maximum hydrogen bonds formed, the further added water then acted more as a medium of blends, so 30% water contents showed an interesting point. The MEA blend shows a different trend from this point, with diffusivity increasing along with the blends changing from 30 to 70% w/w water contents. This trend is different from that of two diamine blends. This may be caused by the polarity change of the property of blend medium toward that of water. The higher polarity of the medium assisted the shift of a more polar MEA molecule, resulting in a climbing diffusivity curve. The increasing medium polarity had little impact on the diamines with lower polarity, so their diffusivity curves were generally

steady in this range. Therefore, the largest diffusivities of two diamine blends were observed in the DMEDA and DMPDA blends without water at 313.0 K (26.34×10^{-10} and $19.44 \times 10^{-10} \text{ m}^2 \cdot \text{s}^{-1}$, respectively), and MEA had its largest diffusivity in the aqueous blend ($7.26 \times 10^{-10} \text{ m}^2 \cdot \text{s}^{-1}$). The maximum diffusivity of two diamines in nonwater blends is higher than that of both MEA nonwater and water blends. Although avoiding the presence of some water is unrealistic under real-world conditions, minimizing the water content can significantly increase the diffusivity in these water-lean blends.

3.1.5. Viscosity. Solution viscosity is an equally important parameter in industrial and engineering applications, given that it is strongly related to the diffusivity of species in solution and is used (as a parameter) to predict the CO₂ mass transfer performance of different absorbent systems. Often a balance between the two properties must be struck given the requirement to pump solutions around the capture process, the size of the pumping equipment to do so increasing with increasing viscosity and becoming limited to a point. Viscosities of the three amine-based absorbent systems at 313.0 K as a function of CO₂ loading have been evaluated here with a summary of the measured data shown graphically in Figure 8.

Viscosities in the aqueous blends of MEA, DMEDA, and DMPDA appear almost linear with increasing CO₂ loading, with a relatively small increase with increasing CO₂ loading. The corresponding blends with NMP increase in an exponential trend with CO₂ loading. This indicates that viscosities of water-lean absorbents are more sensitive to changes in CO₂ loading compared to aqueous absorbents. A similar phenomenon was also observed in the diffusivities where hydrogen bonding is also a key factor for the viscosity of solution. Interestingly, reduction of water content has a larger impact on the solution viscosity in the MEA blends going from a completely aqueous system to those in the presence of NMP despite their lower molecular weight compared to DMEDA and DMPDA. Below a CO₂ loading of 0.4, the MEA blends containing NMP are very similar. Above a loading of 0.4, the viscosity increases with decreasing water content. This is different to the DMEDA and DMPDA blends containing NMP, in which the viscosity increases with increasing water content across all CO₂ loadings. This can be attributed to the hydroxyl group of MEA, which has a stronger interaction than the amino group of two diamines with the carbamate formed in the reaction.

3.2. Hydrodynamic Radius. The diffusion of particles through a liquid with low Reynolds number is governed by the

Stokes–Einstein equation as shown in eq 2, with the assumption that the particle is represented as a sphere of hydrodynamic radius r (Å).

$$D = \frac{k_B T}{6\pi\eta r} \quad (2)$$

$$k = \frac{k_B}{6\pi r} \quad (3)$$

Plotting the measured diffusion coefficient D ($\text{m}^2\cdot\text{s}^{-1}$) versus the ratio of temperature to the measured viscosity T/η ($\text{K}\cdot(\text{Pa}\cdot\text{s})^{-1}$) will provide a linear relationship proportional to the inverse of the hydrodynamic radius r for species in solution, which do not undergo any change to their hydrodynamic radii via processes such as aggregation. Linearity across the data evaluated for each of the amine absorbents at 293.0 K is shown in Figure 9, indicating that each of the species remains

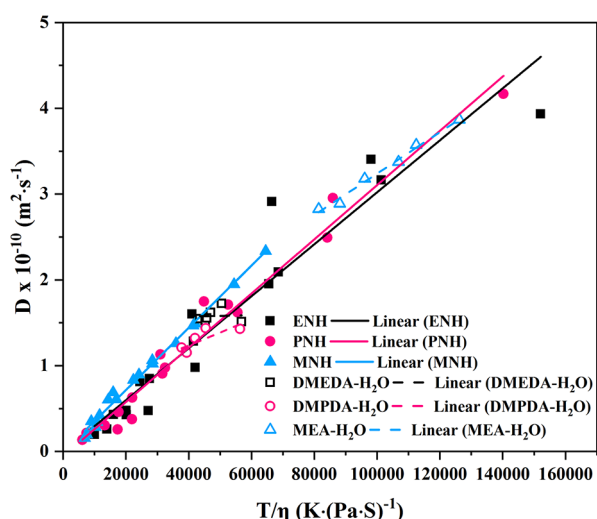


Figure 9. Plot of diffusivity (D) versus the ratio T/η for each amine in the water-lean and aqueous absorbents at 293.0 K.

unimolecular across the conditions studied. A similar relationship was also found for the data at 313.0 K. Under these conditions, the hydrodynamic radii of each species can be calculated by the linear slope k , as shown in eq 3.

Calculated hydrodynamic radii for each of the species H_2O , NMP, amine, and carbamate at 293.0 and 313.0 K are summarized in Table 2 and shown in Figure 10. The same y-axis maximum of 5.0 Å is adopted in Figure 10 so that the height of the bars illustrates the relative hydrodynamic radii. The magnitude of the hydrodynamic radii generally reflects the spatial size of the species with the trend in the data here following carbamate > amine > NMP > water. The most noticeable difference across all the datasets was that the hydrodynamic radii decreased significantly at higher temperature in the water-lean blends but conversely were unaffected in the aqueous absorbents. It is possible that weaker molecular interactions between water, amine, and carbamate with NMP are significantly reduced at higher temperature, while the stronger H-bonding interactions with water are less affected. This would then lead to a relatively larger increase in diffusivity at elevated temperature for the water-lean absorbents compared to aqueous absorbents.

The hydrodynamic radii of the amines were similar in all water-lean absorbents at 293.0 K (2.0–2.4 Å) but were smaller

Table 2. Hydrodynamic Radii of Different Species in Water-Lean and Aqueous Absorbents

	293.0 K			313.0 K			
	water	r_H (Å)	R^2	std. error	r_H (Å)	R^2	std. error
ENH		1.6	0.94	0.1	1.16	0.97	0.05
PNH		1.6	0.89	0.2	1.14	0.94	0.07
MNH		1.38	0.97	0.06	1.16	0.97	0.05
DMEDA-H ₂ O		0.64	0.98	0.04	0.71	0.99	0.04
DMPDA-H ₂ O		0.63	0.94	0.08	0.7	0.91	0.1
MEA-H ₂ O		1.7	0.99	0.1	1.38	0.99	0.07
293.0 K							
NMP	r_H (Å)	R^2	std. error	r_H (Å)	R^2	std. error	
ENH	1.9	0.92	0.1	1.34	0.96	0.07	
PNH	1.8	0.92	0.1	1.24	0.98	0.05	
MNH	1.64	0.96	0.08	1.27	0.96	0.06	
293.0 K							
amine	r_H (Å)	R^2	std. error	r_H (Å)	R^2	std. error	
ENH	2.4	0.97	0.1	1.48	0.97	0.07	
PNH	2.38	0.99	0.07	1.56	0.98	0.06	
MNH	2.04	1.00	0.02	1.47	0.95	0.08	
DMEDA-H ₂ O	2.3	0.99	0.1	2.08	1.00	0.04	
DMPDA-H ₂ O	2.5	0.99	0.1	2.26	1.00	0.03	
MEA-H ₂ O	2.28	1.00	0.04	1.78	1.00	0.04	
293.0 K							
carbamate	r_H (Å)	R^2	std. error	r_H (Å)	R^2	std. error	
ENH	4.3	0.97	0.2	1.8	0.95	0.1	
PNH	4.7	0.96	0.3	2.2	0.98	0.1	
MNH	4.2	0.99	0.1	2.73	0.99	0.06	
DMEDA-H ₂ O	2.76	1.00	0.05	2.62	1.00	0.05	
DMPDA-H ₂ O	2.91	1.00	0.04	2.79	1.00	0.04	
MEA-H ₂ O	3.11	1.00	0.05	2.48	1.00	0.03	

in the water-lean absorbents at 313.0 K (1.5–1.6 Å). This is similarly advantageous alongside the diffusivity, and the amine as the reactive species will have a positive effect on CO_2 mass transfer. Unsurprisingly, the carbamates of all three amines had the largest hydrodynamic radii in the water-lean absorbents at 293.0 K (4.2–4.7 Å), decreasing dramatically at 313.0 K (1.8–2.7 Å). Conversely, they remained constant in the aqueous absorbents. This is consistent with the theory that the interaction with NMP is weaker at higher temperature. This reduction in hydrodynamic radius with increased temperature of the carbamates in the water-lean absorbents is also advantageous as the resulting increased diffusivity allows this product of the reaction between CO_2 and amine to more rapidly move away from the gas–liquid interface and into the bulk solution, which would also positively impact CO_2 mass transfer.

The difference in hydrodynamic radii between the water-lean and aqueous absorbents for each of the amines was consistent apart from the hydrodynamic radius of H_2O in the aqueous blends, which was notably larger in the aqueous MEA absorbent. This further supports the stronger hydrogen bonding characteristics of MEA, via the hydroxyl group, with H_2O . The effect was weakened in the presence of NMP.

4. CONCLUSIONS

Diffusivities in three water-lean absorbent systems comprising the diamines DMEDA and DMPDA and alkanolamine MEA with NMP as an organic diluent, together with their

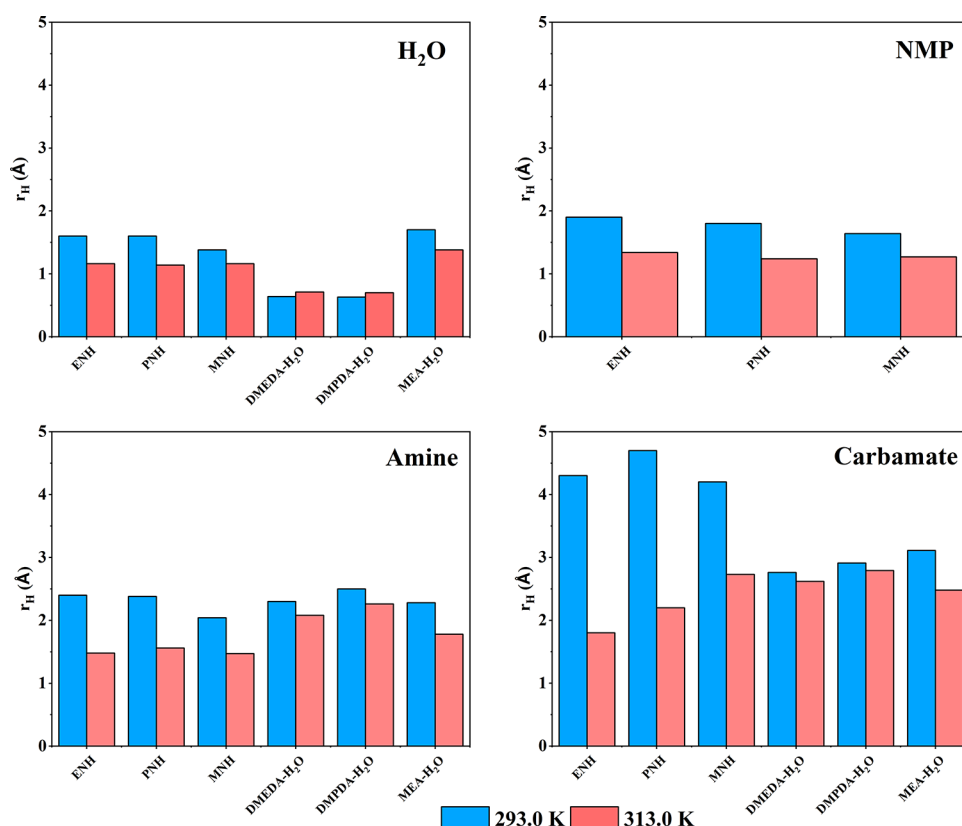


Figure 10. Hydrodynamic radii of species in different solvent systems.

corresponding aqueous absorbents, were investigated here using a convenient and reproducible NMR analysis technique. Diffusivities of the four main species in the absorbent systems, H₂O, NMP, amine, and carbamate, were determined. The influence of several properties including temperature, CO₂ loading, absorbent composition, and viscosity on diffusivity of the species in the blends was determined.

The diffusion coefficients and viscosities were found to be very dependent upon CO₂ content in the water-lean absorbent blends and much less so in the aqueous blends. It was also found that the water and NMP fractions had a significant impact on diffusivities, with diffusivity in the diamine blends decreasing with increasing water, while the MEA blends passed through a minimum with water content. This suggests that mass transfer benefits can be obtained by minimizing the water content of water-lean absorbents.

The resulting dataset of diffusion coefficients was observed to follow a linear relationship with the ratio of temperature and viscosity (T/η) in accordance with the Stokes–Einstein equation. This allowed the estimation of the hydrodynamic radius r_H of each species as a function of composition. It was found that in the water-lean absorbent blends, r_H values of the components decreased with increased temperature, while in the aqueous blends, they remained relatively unchanged. This was attributed to the presence of NMP weakening intermolecular interactions between molecules relative to water and its ability to form strong hydrogen bonds. These weaker interactions are further reduced by increasing the temperature. This suggests that r_H , and by relationship, the diffusivity, is more sensitive to temperature in water-lean absorbents with significant increases in diffusivity due to small temperature increases compared to the aqueous absorbent. As

a consequence, the optimal operating conditions to maximize mass transfer will be different in water-lean and aqueous absorbent systems.

ASSOCIATED CONTENT

Supporting Information

The Supporting Information is available free of charge at <https://pubs.acs.org/doi/10.1021/acs.iecr.2c01990>.

Compositions and abbreviations of water-lean absorbents and their blends; diffusion coefficient of species versus CO₂ loading at different temperatures in DMEDA-based, DMPDA-based, and MEA-based absorbents (PDF)

AUTHOR INFORMATION

Corresponding Authors

Tao Wang – State Key Laboratory of Clean Energy Utilization, Zhejiang University, Hangzhou 310027, P.R. China; orcid.org/0000-0002-0535-7821; Email: oatgnaw@zju.edu.cn

Roger J. Mulder – CSIRO Manufacturing, Clayton, VIC 3168, Australia; orcid.org/0000-0002-8740-802X; Email: Roger.Mulder@csiro.au

Authors

Yanjie Xu – State Key Laboratory of Clean Energy Utilization, Zhejiang University, Hangzhou 310027, P.R. China; CSIRO Manufacturing, Clayton, VIC 3168, Australia; orcid.org/0000-0002-6737-8222

Qi Yang – CSIRO Manufacturing, Clayton, VIC 3168, Australia

Graeme Puxty – CSIRO Energy, Mayfield West, NSW 2304, Australia; orcid.org/0000-0002-6880-7594

Hai Yu – CSIRO Energy, Mayfield West, NSW 2304, Australia; orcid.org/0000-0002-4552-9552

William Conway – CSIRO Energy, Mayfield West, NSW 2304, Australia; orcid.org/0000-0002-7958-3872

Mengxiang Fang – State Key Laboratory of Clean Energy Utilization, Zhejiang University, Hangzhou 310027, P.R. China

Complete contact information is available at:

<https://pubs.acs.org/10.1021/acs.iecr.2c01990>

Notes

The authors declare no competing financial interest.

ACKNOWLEDGMENTS

The authors acknowledge financial support from the National Key R&D Program of China (no. 2017YFB0603300), Zhejiang Provincial Natural Science Foundation of China (grant number LR19E060002), and CSIRO Energy.

ABBREVIATIONS

AMP	2-amino-2-methylpropanol
CCUS	carbon capture, utilization, and storage
CO ₂ BOL	CO ₂ -binding organic liquids
DETA	diethylenetriamine
DMEDA	N,N-dimethyl-1,2-ethanediamine
DMPDA	N,N-dimethyl-1,3-propanediamine
MDEA	N-methyldiethanolamine
MEA	monoethanolamine
NMP	N-methyl-2-pyrrolidone
PZ	piperazine
SFL	sulfolane

REFERENCES

- (1) Friedlingstein, P.; O'Sullivan, M.; Jones, M. W.; Andrew, R. M.; Hauck, J.; Olsen, A.; Peters, G. P.; Peters, W.; Pongratz, J.; Sitch, S.; Le Quéré, C.; Canadell, J. G.; Ciais, P.; Jackson, R. B.; Alin, S.; Aragão, L. E. O. C.; Arneth, A.; Arora, V.; Bates, N. R.; Becker, M.; Benoit-Cattin, A.; Bittig, H. C.; Bopp, L.; Bultan, S.; Chandra, N.; Chevallier, F.; Chini, L. P.; Evans, W.; Florentie, L.; Forster, P. M.; Gasser, T.; Gehlen, M.; Gilfillan, D.; Gkrizalis, T.; Gregor, L.; Gruber, N.; Harris, I.; Hartung, K.; Haverd, V.; Houghton, R. A.; Ilyina, T.; Jain, A. K.; Joetzer, E.; Kadono, K.; Kato, E.; Kitidis, V.; Korsbakken, J. I.; Landschützer, P.; Lefèvre, N.; Lenton, A.; Lienert, S.; Liu, Z.; Lombardozzi, D.; Marland, G.; Metzl, N.; Munro, D. R.; Nabel, J. E. M. S.; Nakaoaka, S. I.; Niwa, Y.; O'Brien, K.; Ono, T.; Palmer, P. I.; Pierrot, D.; Poultar, B.; Resplandy, L.; Robertson, E.; Rödenbeck, C.; Schwaner, J.; Séférian, R.; Skjelvan, I.; Smith, A. J. P.; Sutton, A. J.; Tanhua, T.; Tans, P. P.; Tian, H.; Tilbrook, B.; Van Der Werf, G.; Vuichard, N.; Walker, A. P.; Wanninkhof, R.; Watson, A. J.; Willis, D.; Wiltshire, A. J.; Yuan, W.; Yue, X.; Zaehle, S. Global Carbon Budget 2020. *Earth Syst. Sci. Data* **2020**, *12*, 3269–3340.
- (2) Broeder, P.; Svendsen, H. F. Capacity and Kinetics of Solvents for Post-Combustion CO₂ Capture. *Energy Procedia* **2012**, *23*, 45–54.
- (3) Ma'mum, S.; Svendsen, H. F.; Hoff, K. A.; Juliussen, O. Selection of New Absorbents for Carbon Dioxide Capture. *Greenhouse Gas Control Technol.* **7** *2005*, *48*, 45–53.
- (4) Zhang, J.; Misch, R.; Tan, Y.; Agar, D. W. Novel Thermomorphic Biphasic Amine Solvents for CO₂ Absorption and Low-Temperature Extractive Regeneration. *Chem. Eng. Technol.* **2011**, *34*, 1481–1489.
- (5) Oh, S. Y.; Binns, M.; Cho, H.; Kim, J. K. Energy Minimization of MEA-Based CO₂ Capture Process. *Appl. Energy* **2016**, *169*, 353–362.
- (6) Xue, B.; Yu, Y.; Chen, J.; Luo, X.; Wang, M. A Comparative Study of MEA and DEA for Post-Combustion CO₂ Capture with Different Process Configurations. *Int. J. Coal Sci. Technol.* **2017**, *4*, 15–24.
- (7) Nguyen, T.; Hilliard, M.; Rochelle, G. Volatility of Aqueous Amines in CO₂ Capture. *Energy Procedia* **2011**, *4*, 1624–1630.
- (8) Budzianowski, W. M. *Green Energy and Technology Energy Efficient Solvents for CO₂ Capture by Gas-Liquid Absorption Compounds, Blends and Advanced Solvent Systems*; Springer: 2017.
- (9) Li, L.; Voice, A. K.; Li, H.; Namjoshi, O.; Nguyen, T.; Du, Y.; Rochelle, G. T. Amine Blends Using Concentrated Piperazine. *Energy Procedia* **2013**, *37*, 353–369.
- (10) Gaspar, J.; Thomsen, K.; Von Solms, N.; Fosbøl, P. L. Solid Formation in Piperazine Rate-Based Simulation. *Energy Procedia* **2014**, *63*, 1074–1083.
- (11) Kim, I.; Ma, X.; Andreassen, J. P. Study of the Solid-Liquid Solubility in the Piperazine-H₂O-CO₂ System Using FBRM and PVM. *Energy Procedia* **2012**, *23*, 72–81.
- (12) Lani, B.; Dombrowski, K. D. *Evaluation of Concentrated Piperazine for CO₂ Capture from Coal-Fired Flue Gas Background*; URS Group, Inc.: Austin, TX. 2010.
- (13) Henni, A.; Mather, A. E. Solubility of Carbon Dioxide in Methyldiethanolamine + Methanol + Water. *J. Chem. Eng. Data* **1995**, *40*, 493–495.
- (14) Tan, J.; Shao, H.; Xu, J.; Du, L.; Luo, G. Mixture Absorption System of Monoethanolamine-Triethylene Glycol for CO₂ Capture. *Ind. Eng. Chem. Res.* **2011**, *50*, 3966–3976.
- (15) Choi, Y. S.; Im, J.; Jeong, J. K.; Hong, S. Y.; Jang, H. G.; Cheong, M.; Lee, J. S.; Kim, H. S. CO₂ Absorption and Desorption in an Aqueous Solution of Heavily Hindered Alkanolamine: Structural Elucidation of CO₂-Containing Species. *Environ. Sci. Technol.* **2014**, *48*, 4163–4170.
- (16) Chen, S.; Chen, S.; Zhang, Y.; Chai, H.; Qin, L.; Gong, Y. An Investigation of the Role of N-Methyl-Diethanolamine in Non-Aqueous Solution for CO₂ Capture Process Using ¹³C NMR Spectroscopy. *Int. J. Greenhouse Gas Control* **2015**, *39*, 166–173.
- (17) Yuan, Y.; Rochelle, G. T. CO₂ Absorption Rate in Semi-Aqueous Monoethanolamine. *Chem. Eng. Sci.* **2018**, *182*, 56–66.
- (18) Svensson, H.; Edfeldt, J.; Zejnnullahu Velasco, V.; Hulteberg, C.; Karlsson, H. T. Solubility of Carbon Dioxide in Mixtures of 2-Amino-2-Methyl-1-Propanol and Organic Solvents. *Int. J. Greenhouse Gas Control* **2014**, *27*, 247–254.
- (19) Tan, L. S.; Shariff, A. M.; Lau, K. K.; Bustam, M. A. Impact of High Pressure on High Concentration Carbon Dioxide Capture from Natural Gas by Monoethanolamine/N-Methyl-2-Pyrrolidone Solvent in Absorption Packed Column. *Int. J. Greenhouse Gas Control* **2015**, *34*, 25–30.
- (20) Pakzad, P.; Mofarahi, M.; Izadpanah, A. A.; Afkhamipour, M.; Lee, C. H. An Experimental and Modeling Study of CO₂ Solubility in a 2-Amino-2-Methyl-1-Propanol (AMP) + N-Methyl-2-Pyrrolidone (NMP) Solution. *Chem. Eng. Sci.* **2018**, *175*, 365–376.
- (21) Kortunov, P.; Baugh, L. S.; Calabro, D. C.; Siskin, M. High CO₂ to Amine Adsorption Capacity CO₂ Scrubbing Processes. U.S. Patent No. 9,028,785 Google Patents May 12, 2015.
- (22) Wang, L.; Yu, S.; Li, Q.; Zhang, Y.; An, S.; Zhang, S. Performance of Sulfolane/DETA Hybrids for CO₂ Absorption: Phase Splitting Behavior, Kinetics and Thermodynamics. *Appl. Energy* **2018**, *228*, 568–576.
- (23) Jenab, M. H.; Abdi, M. A.; Najibi, S. H.; Vahidi, M.; Matin, N. S. Solubility of Carbon Dioxide in Aqueous Mixtures of N-Methyldiethanolamine + Piperazine + Sulfolane. *J. Chem. Eng. Data* **2005**, *50*, 583–586.
- (24) Li, H.; Guo, H.; Shen, S. Low-Energy-Consumption CO₂Capture by Liquid-Solid Phase Change Absorption Using Water-Lean Blends of Amino Acid Salts and 2-Alkoxyethanols. *ACS Sustainable Chem. Eng.* **2020**, *8*, 12956–12967.
- (25) Bihong, L.; Kexuan, Y.; Xiaobin, Z.; Zuoming, Z.; Guohua, J. 2-Amino-2-Methyl-1-Propanol Based Non-Aqueous Absorbent for

- Energy-Efficient and Non-Corrosive Carbon Dioxide Capture. *Appl. Energy* **2020**, *264*, No. 114703.
- (26) Heldebrant, D. J.; Yonker, C. R.; Jessop, P. G.; Phan, L. CO₂-Binding Organic Liquids (CO₂ BOLs) for Post-Combustion CO₂ Capture. *Energy Procedia* **2009**, *1*, 1187–1195.
- (27) Mathias, P. M.; Afshar, K.; Zheng, F.; Bearden, M. D.; Freeman, C. J.; Andrea, T.; Koehl, P. K.; Kutnyakov, I.; Zwoster, A.; Smith, A. R.; Jessop, P. G.; Nik, O. G.; Heldebrant, D. J. Improving the Regeneration of CO₂-Binding Organic Liquids with a Polarity Change. *Energy Environ. Sci.* **2013**, *6*, 2233–2242.
- (28) Gonzalez-Miquel, M.; Bedia, J.; Abrusci, C.; Palomar, J.; Rodriguez, F. Anion Effects on Kinetics and Thermodynamics of CO₂ Absorption in Ionic Liquids. *J. Phys. Chem. B* **2013**, *117*, 3398–3406.
- (29) Galán Sánchez, L. M.; Meindersma, G. W.; de Haan, A. B. Kinetics of Absorption of CO₂ in Amino-Functionalized Ionic Liquids. *Chem. Eng. J.* **2011**, *166*, 1104–1115.
- (30) Zubeir, L. F.; Nijssen, T. M. J.; Spyriouni, T.; Meuldijk, J.; Hill, J. R.; Kroon, M. C. Carbon Dioxide Solubilities and Diffusivities in 1-Alkyl-3-Methylimidazolium Tricyanomethide Ionic Liquids: An Experimental and Modeling Study. *J. Chem. Eng. Data* **2016**, *61*, 4281–4295.
- (31) Liu, A. H.; Li, J. J.; Ren, B. H.; Lu, X. B. Development of High-Capacity and Water-Lean CO₂ Absorbents by a Concise Molecular Design Strategy through Viscosity Control. *ChemSusChem* **2019**, *12*, 5164–5171.
- (32) Amundsen, T. G.; Øi, L. E.; Eimer, D. A. Density and Viscosity of Monoethanolamine + Water + Carbon Dioxide from (25 to 80) °C. *J. Chem. Eng. Data* **2009**, *54*, 3096–3100.
- (33) Xu, Y.; Wang, T.; Yang, Q.; Yu, H.; Fang, M.; Puxty, G. CO₂ Absorption Performance in Advanced Water-Lean Diamine Solvents. *Chem. Eng. J.* **2021**, *425*, No. 131410.
- (34) Xu, Y.; Fang, M.; Yang, Q.; Xia, Z.; Yu, H.; Wang, T.; Chen, K.; Puxty, G. Diamine Based Water-Lean CO₂ Solvent with Extra High Cyclic Capacity and Low Viscosity. *Greenhouse Gases Sci. Technol.* **2021**, *11*, 828–836.
- (35) Gonzalez-Miquel, M.; Bedia, J.; Palomar, J.; Rodriguez, F. Solubility and Diffusivity of CO₂ in [Hxmim][NTf₂], [Omim]-[NTf₂], and [Dcmim][NTf₂] at T = (298.15, 308.15, and 323.15) K and Pressures up to 20 Bar. *J. Chem. Eng. Data* **2014**, *59*, 212–217.
- (36) Moya, C.; Palomar, J.; Gonzalez-Miquel, M.; Bedia, J.; Rodriguez, F. Diffusion Coefficients of CO₂ in Ionic Liquids Estimated by Gravimetry. *Ind. Eng. Chem. Res.* **2014**, *53*, 13782–13789.
- (37) Shiflett, M. B.; Yokozeki, A. Solubilities and Diffusivities of Carbon Dioxide in Ionic Liquids: [Bmim][PF₆] and [Bmim][BF₄]. *Ind. Eng. Chem. Res.* **2005**, *44*, 4453–4464.
- (38) Moganty, S. S.; Baltus, R. E. Diffusivity of Carbon Dioxide in Room-Temperature Ionic Liquids. *Ind. Eng. Chem. Res.* **2010**, *49*, 9370–9376.
- (39) Hou, Y.; Baltus, R. E. Experimental Measurement of the Solubility and Diffusivity of CO₂ in Room-Temperature Ionic Liquids Using a Transient Thin-Liquid-Film Method. *Ind. Eng. Chem. Res.* **2007**, *46*, 8166–8175.
- (40) Kortenbruck, K.; Pohrer, B.; Schlueter, E.; Friedel, F.; Ivanovic-Burmazovic, I. Determination of the Diffusion Coefficient of CO₂ in the Ionic Liquid EMIM NTf₂ Using Online FTIR Measurements. *J. Chem. Thermodyn.* **2012**, *47*, 76–80.
- (41) Snijder, E. D.; te Riele, M. J. M.; Versteeg, G. F.; van Swaaij, W. P. M. Diffusion Coefficients of Several Aqueous Alkanolamine Solutions. *J. Chem. Eng. Data* **1993**, *38*, 475–480.
- (42) Liu, F.; Chen, S.; Gao, Y. Synthesis of Porous Polymer Based Solid Amine Adsorbent: Effect of Pore Size and Amine Loading on CO₂ Adsorption. *J. Colloid Interface Sci.* **2017**, *506*, 236–244.
- (43) Kudahi, S. N.; Noorpoor, A. R.; Mahmoodi, N. M. Determination and Analysis of CO₂ Capture Kinetics and Mechanisms on the Novel Graphene-Based Adsorbents. *J. CO₂ Util.* **2017**, *21*, 17–29.
- (44) MacDonald, T. S. C.; Price, W. S.; Beves, J. E. Time-Resolved Diffusion NMR Measurements for Transient Processes. *ChemPhysChem* **2019**, *20*, 926–930.
- (45) Masaro, L.; Baille, W. E.; Zhu, X. X. Interaction of Ethylene Glycol with Poly(Vinyl Alcohol) in Aqueous Systems as Studied by NMR Spectroscopy. *Am. Chem. Soc. Polym. Prepr. Div. Polym. Chem.* **2000**, *41*, 62–63.
- (46) Price, W. S. Pulsed-Field Gradient Nuclear Magnetic Resonance as a Tool for Studying Translational Diffusion, Part 1: Basic Theory. *Concepts Magn. Reson.* **1997**, *9*, 299–336.
- (47) Price, W. S. Pulsed-Field Gradient Nuclear Magnetic Resonance as a Tool for Studying Translational Diffusion: Part II. Experimental Aspects. *Concepts Magn. Reson.* **1998**, *10*, 197–237.
- (48) Gilliland, E. R. Diffusion Coefficients in Gaseous Systems. *Ind. Eng. Chem.* **1934**, *26*, 681–685.
- (49) Sadakiyo, M.; Yamada, T.; Kitagawa, H. Hydroxyl Group Recognition by Hydrogen-Bonding Donor and Acceptor Sites Embedded in a Layered Metal - Organic Framework. *J. Am. Chem. Soc.* **2011**, *133*, 11050–11053.

□ Recommended by ACS

Study on the Oil Displacement Mechanism of Different SP Binary Flooding Schemes for a Conglomerate Reservoir Based on a Microfluidic Model

Fengqi Tan, Chaoliang Zhang, et al.

MARCH 27, 2023

INDUSTRIAL & ENGINEERING CHEMISTRY RESEARCH

READ ▶

Analysis of Different Organic Rankine and Kalina Cycles for Waste Heat Recovery in the Iron and Steel Industry

Davood Atashbozorg, Masoud Torabi Azad, et al.

DECEMBER 06, 2022

ACS OMEGA

READ ▶

Evaluation of a Third Generation Single-Component Water-Lean Diamine Solvent for Post-Combustion CO₂ Capture

Dushyant Barpaga, David J. Heldebrant, et al.

MARCH 29, 2022

ACS SUSTAINABLE CHEMISTRY & ENGINEERING

READ ▶

Technical, Economical, and Environmental Performance Assessment of an Improved Triethylene Glycol Dehydration Process for Shale Gas

Gaihuan Liu, Huimin Liu, et al.

JANUARY 04, 2022

ACS OMEGA

READ ▶

Get More Suggestions >